Water Practice & Technology

IWA PUBLISHING

Water Practice & Technology Vol 18 No 10, 2372 doi: 10.2166/wpt.2023.148

Development of flood inundation maps for the Chaliyar Basin, Kerala under climate change scenarios

Nagireddy Venkata Jayasimha Reddy and R. Arunkumar *

Department of Civil Engineering, National Institute of Technology Calicut, Kozhikode, Kerala 673601, India
*Corresponding author. E-mail: arunkr@nitc.ac.in

RA, 0000-0002-4211-7480

ABSTRACT

Floods are one of the extreme events and widespread natural disasters that significantly affect the civil infrastructure and livelihoods of people. Recently, climate change has significantly altered the rainfall pattern and increased flood events worldwide, especially in India. Therefore, it has become essential to map potential flood inundation regions for various future extreme events to develop appropriate flood mitigation and management strategies. This study aims to develop flood inundation maps for different return periods under climate change scenarios for the Chaliyar basin, Kerala. The Hydrologic Engineering Center-Hydrologic Modelling System model was used to simulate streamflow under SSP2-4.5 and SSP5-8.5 scenarios. Later, flood inundation maps were developed for different return periods using the Hydrologic Engineering Center-River Analysis System model. It was observed that for the near future (2031–2040) and far future (2071–2080), simulated streamflow is higher for SSP5-8.5. However, the mid-future (2051–2060) resulted in a higher streamflow for SSP2-4.5 than the SSP5-8.5 scenario. A maximum of 19.52 m of water surface elevation occurred at Kizhupparamba during mid-future for SSP2-4.5, followed by 18.38 m of water surface elevation at Cheekode during the near future for SSP5-8.5, for 100-year return period events. This study showed that hydrologic and hydraulic models could be effectively combined for mapping the flood inundation areas.

Key words: flood mapping, HEC-HMS, HEC-RAS, SSP scenarios

HIGHLIGHTS

- This study integrates the hydrological model, hydraulic model and climate change scenarios to develop flood inundation maps for various return periods.
- SSP2-4.5 and SSP5-8.5 are considered for climate change scenarios to simulate the streamflow for the near future (2031–2040), mid-future (2051–2060) and far future (2071–2080).
- Future streamflow in the Chaliyar basin will likely to increase for both SSP2-4.5 and SSP5-8.5 scenarios.

1. INTRODUCTION

A flood is a high volume of water flow that rises and drowns the land which is otherwise not normally inundated. It is one of the most prevalent and widespread natural disasters in tropical nations like India, causing havoc on civil infrastructure and people's livelihoods (Mishra *et al.* 2018). It is widely reported that the climate is changing and that this change is already having an impact on every part of the world (Eum *et al.* 2011). As a result of climate change, the global average temperature is increasing, and the rainfall intensity and frequency have also increased. Consequently, the runoff and peak discharge have also increased, leading to flooding in many places. The impact of climate change on floods is severe in Indian river basins, especially in the low-lying floodplains, due to an increase in extreme rainfall events (Ramachandran *et al.* 2019). To identify the flood risk zones and to formulate effective flood mitigation and management strategies, it is crucial to map the possible flood inundation regions for a wide range of extreme rainfall events under climate change scenarios (Sahoo & Sreeja 2017; Hamdan *et al.* 2021; Kalra *et al.* 2021; Mohanty & Simonovic 2021).

The outputs of the general circulation models (GCMs) project future climate for different emission scenarios and are widely used in hydrological modelling to assess climate change's impact. Several studies have used the statistically downscaled GCM projections to simulate hydrological models and analyse the potential

implications of climate change to a basin or sub-basin (Aich *et al.* 2016; Shrestha & Lohpaisankrit 2017; Nyaupane *et al.* 2018; Reshma & Arunkumar 2023). Similarly, flood inundation maps can also be developed by giving these GCM projections as input to an appropriate hydrological or hydraulic model. Hydrological models are simplified replications of the hydrologic cycle (Motovilov *et al.* 1999). Hydrological modelling at the river basin scale is essential to simulate the stream flows and predict floods under various climate change scenarios (Mohammed *et al.* 2018; Siddique & Palmer 2021; Wen *et al.* 2021). A few studies have been reported for mapping floodplains for future climate change scenarios (Shrestha & Lohpaisankrit 2017; Roy *et al.* 2021; Ukumo *et al.* 2022). El Alfy (2016) estimated the peak flows and abstraction losses by integrating the Hydrologic Engineering Center-Hydrologic Modelling System (HEC-HMS) model with geographic information system (GIS) to assess the flash floods. A similar study was conducted by El-Naqa & Jaber (2018) integrating the Hydrologic Engineering Center-River Analysis System (HEC-RAS) model and GIS to map the inundated areas along the main Wadi of Al-Ghadaf watershed for various return periods. It was reported the water level in some places in the inundated areas reached as high as 5 m. Abdessamed & Abderrazak (2019) used both HEC-HMS and HEC-RAS to assess the flood risk for different return periods. It was reported that the presence of retaining walls reduced the area from flooding, however, extremely low-lying regions were at risk of flooding. Using the MIKE 11 model, Rahman *et al.* (2011) investigated the flood flows and associated stages for various return periods for the Teesta sub-catchment in Bangladesh. The model results were used to create a stage–discharge relationship that was used to calculate the flood stages for 25-, 50-, and 100-year return periods.

Climate change has significantly altered the rainfall pattern and increased flood events across the world, especially in India. Therefore, it has become essential to map the potential flood inundation regions for various future extreme rainfall events and identify the flood risk zones for developing appropriate flood mitigation and management strategies. Madhuri *et al.* (2021) studied the flood depth, building risk and the effectiveness of various flood adaption measures for urban floods under climate change scenarios. For the Sebeya catchment, Assoumpta & Aja (2021) used quantitative precipitation forecasts to assess flood predictions. Roy *et al.* (2021) used open-source mathematical models to map the flood inundation of the Arial Khan River for the projected climate change scenario RCP 8.5. Ukumo *et al.* (2022) prepared a flood hazard map for the Woybo River catchment under climate change scenarios. The floods for future periods under different climatic scenarios were simulated using the HEC-RAS model. It was reported that 25.68% of the Woybo River catchment fell into the very high-hazard category, while 28.56% fell into the high-hazard category. From these studies, it is evident that flood mapping is mostly done by integrating hydrological and hydraulic models. Streamflows are simulated using a hydrologic model, whereas flood inundation areas and inundation depth are estimated using a hydraulic model. During the 2018 monsoon, Kerala experienced unusually heavy rainfall. As a result, 13 out of 14 districts experienced severe floods. The Chaliyar basin is one of the severely affected basins in Kerala due to extreme rainfall events and floods. Therefore, the main objectives of the study are to simulate the future streamflow of the basin for different climate change scenarios using a hydrological model and to develop flood inundation maps for different return periods under climate change scenarios using a hydraulic model. This study effectively combines the hydrologic and hydraulic modelling for mapping the flood inundation areas.

The study area and data are explained in the next section, followed by the methodology adopted for hydrologic modelling, extraction of future precipitation and hydraulic model development. Then, the results of various methods regarding streamflow simulation, performance indices, and flood maps for various return periods are explained. Finally, the conclusions from the results are explained in the last section.

2. STUDY AREA

The present study is carried out in the Chaliyar river basin, Kerala, and its location is shown in Figure 1. The river Chaliyar is the fourth longest river in Kerala, with a total length of 169 km and flows from east to west through the districts of Malappuram and Kozhikode. It originates at an altitude of 2,066 m above sea level in the Elambalari Hills in Gudalur taluk of Nilgiris district in Tamil Nadu and drains into the Lakshadweep sea at Beypore, Kerala. The catchment area of the entire basin is 2,933 km^2, of which 2,545 km^2 are in Kerala and the remaining 388 km^2 are in Tamil Nadu.

The average annual rainfall in the basin is about 3,012 mm. The southwest (June–September) and northeast (October–November) monsoons are the two main rainy seasons. The main four soil types in the river basin are gravelly clay (60.73%), clay (24.56%), gravelly loam (9.85%), and loam (4.86%). Generally, the land use of the basin includes urban, rocky, and water bodies with agricultural land making up approximately 74.26% of

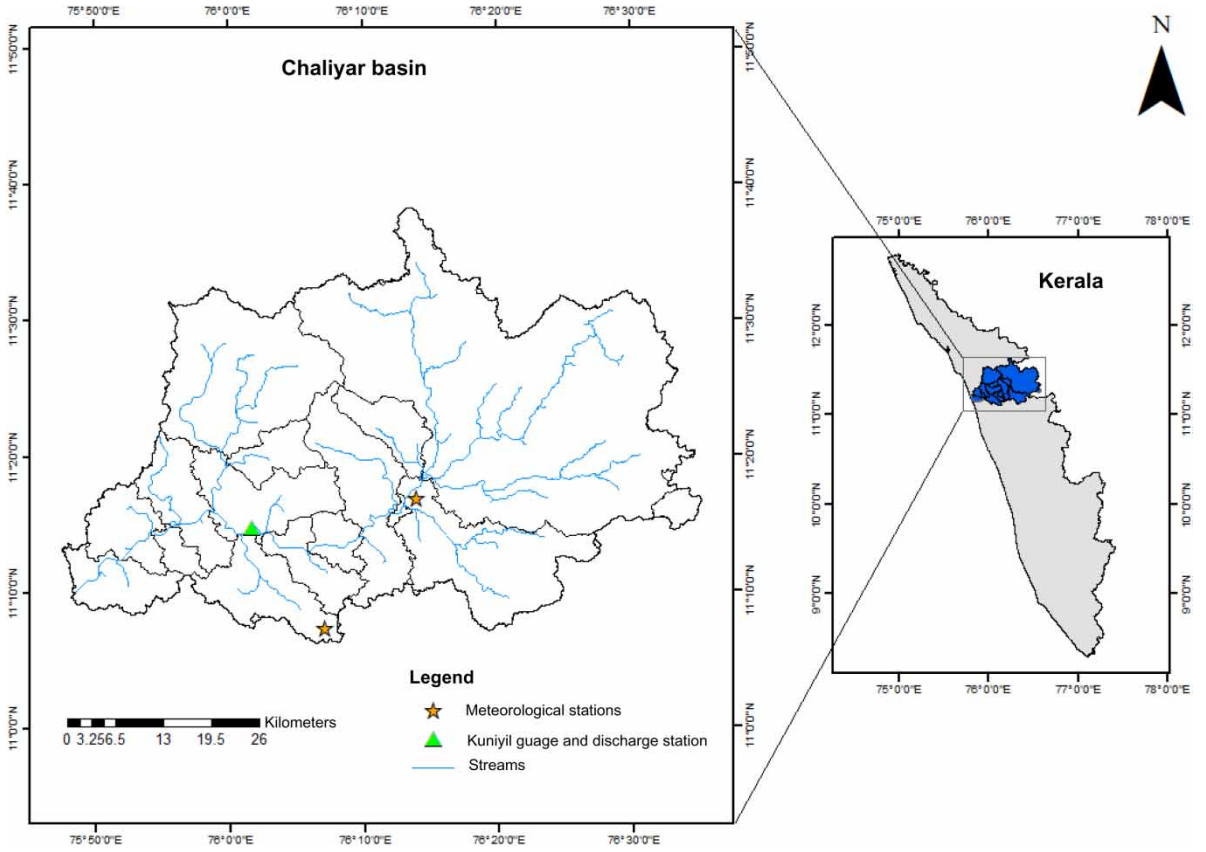

Figure 1 | Location of Chaliyar basin.

the total area and 14.21% forest area. There is a hydrological observation station at Kuniyil and two meteorological stations in the basin located at Nilambur and Manjeri as shown in Figure 1.

The data collected for the study includes the observed daily precipitation for a period of 20 years from 1995 to 2014 from the Indian Meteorological Department (IMD). The digital elevation model (DEM) was obtained from the National Aeronautics and Space Administration (NASA) Earth data Advanced Spaceborne Thermal Emission and Reflection Radiometer (ASTER), and observed daily streamflow (1995–2014) was obtained from Central Water Commission (CWC) through India-WRIS. The land use land cover (LULC) is obtained from United States Geological Survey (USGS) EarthExplorer. The precipitation and temperature projections for the future climate change scenarios were obtained from Mishra *et al.* (2020a). The statistical analysis of historical meteorological and streamflow data from 1995 to 2014 is given in Table 1. As seen from the table, a maximum of 571 mm was observed at Manjeri, whereas the difference in the mean of the two stations is less.

Table 1 | Statistical analysis of historical rainfall and streamflow at Chaliyar basin

Statistic measures	Nilambur rainguage station (mm)	Manjeri rainguage station (mm)	Kuniyil discharge station (m^3/s)
Minimum	0.00	0.00	0.00
Maximum	254.40	571.00	3,256.00
Mean	6.90	7.30	137.00
Skewness	4.40	8.40	4.10
Kurtosis	27.80	168.70	24.30

3. MODEL DEVELOPMENT

The methodology followed in this study is divided into three phases as shown in Figure 2. In phase 1, the HEC-HMS model was developed to simulate the streamflow in the basin for the baseline scenario using the observed historical data. HEC-HMS is a physically based semi-distributed model developed by the Hydrologic Engineering

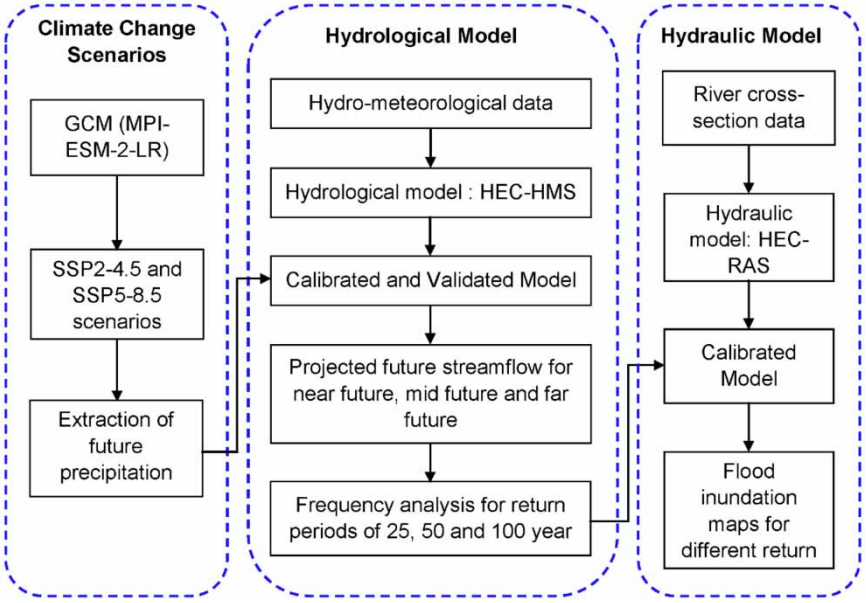

Figure 2 | Flowchart of the overall methodology.

Centre of the US Army Corps of Engineers (Feldman 2021), and is widely used to simulate the streamflow. The main components of the HEC-HMS model are the basin model, meteorological model and control specifications. The inputs for the HEC-HMS model are delineated watershed, daily observed precipitation, sub-basin parameters and observed streamflow. The basin delineated from the ASTER-DEM was imported to the HEC-HMS and the other basin parameters were defined. The basic building blocks of the basin model are its hydrologic components, which include watershed, stream network, and outlet point and are to be represented by an element in HMS. The elements in HMS include sub-basin, reach, reservoir, junction, diversion, source, and sink. Each component is a part of the overall watershed response to a specified atmospheric forcing. In HMS, various methods are available to calculate canopy losses, surface losses, infiltration losses, baseflow, surface runoff estimation, and streamflow routing. The canopy losses were estimated using the simple canopy method, which assumes that all the precipitation is intercepted until the canopy storage capacity is filled. Once the storage is filled, all further precipitation falls to the surface. The simple surface method was used for computing surface losses. The infiltration losses were estimated using the deficit and constant approach and the recession method was used to determine the baseflow. Within the sub-basin, the surface runoff was estimated using a transform approach in which the excess precipitation was converted to runoff using a Clark unit hydrograph. To route the runoff from reaches to sink, the Muskingum method was applied. The model was calibrated with the observed streamflow once the model parameters and control specifications were specified. The performance measures such as the ratio of root mean square error to the standard deviation (RSR), Nash–Sutcliffe efficiency (NSE), coefficient of determination (R^2), and percentage bias (PBIAS) were used to assess the model. Moriasi *et al.* (2007) criteria were further used for rating the model performance.

In the second phase, the bias-corrected climate projections developed by Mishra *et al.* (2020b) from Coupled Model Intercomparison Project-6 (CMIP6) were used in this study for future climate change scenarios. Among 13 GCMs, MPI-ESM-2-LR was selected based on the statistical analysis of the projections with the observed historical data. It has been reported that MPI-ESM-2-LR model precipitation gives good results for Indian climate conditions (Raju & Kumar 2020). To understand the variations in the streamflow, three future time periods, near future (2031–2040), mid-future (2051–2060), and far future (2071–2080) were considered. Flood frequency analysis was used to relate the magnitude of floods to their frequency of occurrence. The Gumbel extreme value distribution was used to develop the extreme flood events for 25-, 50-, and 100-year return periods (Ukumo *et al.* 2022).

In phase 3, flood inundation maps were developed for different return periods for SSP2-4.5 and SSP5-8.5 climate change scenarios using the HEC-RAS model. Coupled one-dimensional (1D) and two-dimensional (2D) HEC-RAS model (Brunner 2016) was used to simulate the water surface elevation and flood extent in the Chaliyar River and adjacent floodplain areas. Hydraulic model parameters of HEC-RAS include river cross-

sections in each sub-basin, including left and right bank locations, roughness coefficients (Manning's n), and contraction and expansion coefficients. The flow hydrographs from HMS were given as the input to the hydraulic (HEC-RAS) model along with the land-use data. For the purpose of constructing the study area terrain model, the terrain's 1/3 arc-second DEM was used. Using RAS Mapper, the DEM of the study region was imported to generate the terrain model for the HEC-RAS 2D steady model. A 2D flow area around the floodplain was constructed using the geometry editor of HEC-RAS based on an estimate of the flood extent. The area was marked off with a polygon, and the flow area around the floodplain was created by taking into account the banks and the probability of flooding along the main channel. The mesh contains 11,280 cells. The cell size used for mesh was 100 m × 100 m square grids. The average width of the channel was 400 m. A floodplain of 1.5 km was considered for mesh generation on both sides of banks as shown in Figure 3. Therefore, the average width of the floodplain is 3 km. The hydraulic properties of each newly formed cell in the RAS Mapper were assigned by running the geometric pre-processor. Additionally, by establishing the land cover grid in GIS, the associated Manning's roughness coefficient n according to the kind of land use was assigned within the 2D flow area (Brunner 2016). The upstream and downstream boundary condition lines were drawn and boundary conditions were provided for the 2D steady flow simulation. HEC-RAS received the flow hydrograph for the upstream and normal depth at downstream as the hydrologic input. Making an accurate assessment of the mesh size, quantity, and computational time is crucial for modelling accuracy. Given this, a computation interval of 10 min was adopted as a moderate interval, and a small cell size was selected for good results even though it would require more time to run the simulation. The conservation of mass and energy equation is the formula utilized in the modelling (Equation (1)).

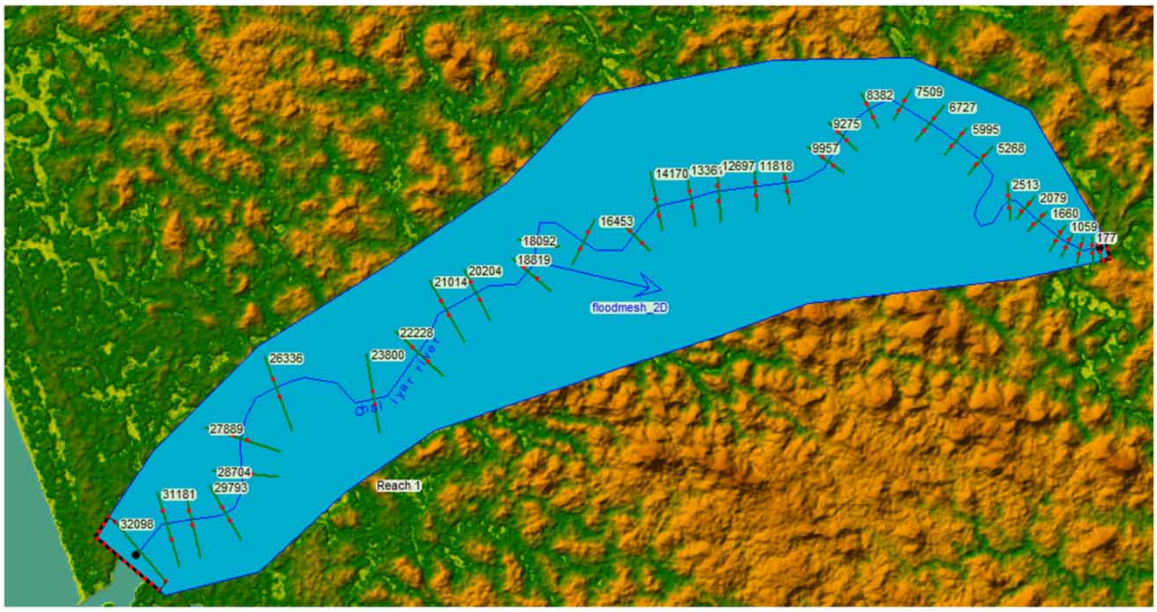

Figure 3 | RAS geometry and the cross-sections at various chainages of the Chaliyar basin.

$$Z_2 + Y_2 + \frac{\alpha_2 v_2^2}{2g} = Z_1 + Y_1 + \frac{\alpha_1 v_1^2}{2g} + h_e \tag{1}$$

where Y_1 and Y_2 are the depths (m) of water at adjoining cross-section 1 and cross-section 2; Z_1 and Z_2 are the elevations (m) of the main channel; V_1 and V_2 are the average velocities (m/s) (total discharge/total flow area); α_1 and α_2 are the velocity weighting coefficients; g is the gravitational acceleration (m/s^2); and h_e is the energy head loss (m).

The diffusion wave technique was utilized for this 2D unsteady model without taking eddy viscosity and Coriolis effects into account (Equation (2)). The mass conservation or continuity equation is used in the unsteady

computation.

$$\frac{\partial H}{\partial t} + \frac{\partial (uh)}{\partial x} + \frac{\partial (vh)}{\partial y} + q = 0 \tag{2}$$

where H is water surface elevation (m); q is the discharge term related to source or sink (m/s); h is the depth of water (m); u and v are the velocity components (m/s) in the X and Y directions.

4. RESULTS AND DISCUSSIONS

In this study, the impact of climate change on streamflow and its subsequent flooding were assessed for various scenarios. The projected precipitation for different emission scenarios was used for the assessment. The HEC-HMS was used to simulate the streamflow for the near future (2031–2040), mid-future (2051–2060), and far future (2071–2080) under SSP2-4.5 and SSP5-8.5 scenarios. The simulated streamflow was then fed into the HEC-RAS model to create the flood maps for various return periods. The results of various models and assessments are discussed in the following sections.

4.1. Hydrological modelling

The values of the model parameter were modified until the observed streamflow and computed streamflow were relatively close to each other. Both manual and automatic calibrations were performed to fine-tune the simulations of the HEC-HMS model. For automatic calibration, simplex and univariate methods were used. The final calibrated values of the model parameters are presented in Table 2. It is observed that the initial storage in the canopy loss, time of concentration and Muskingum parameters are significant streamflow simulations.

Table 2 | Calibrated model parameters of HMS model

Model	Parameter	Initial value	Calibrated value
Canopy	Initial storage	8%	16%
	Maximum storage (mm)	5.2	7
	Crop coefficient	1	0.80
Loss	Initial deficit (mm)	11	4.73
	Maximum deficit (mm)	15	14
	Constant rate (mm/h)	1.14	0.46
Transform	Time of concentration (h)	21	16.33
	Storage coefficient (h)	56	56
Baseflow	Initial discharge (m^3/s)	17	17
	Recession constant	0.90	0.90
	Ratio to peak	0.16	0.42
Routing	K (h)	0.39	0.32
	X	0.41	0.10

Calibration of the HEC-HMS model for streamflow was performed using observed daily streamflow data for 8 years (1995–2002) and validated for 3 years (2011–2013). The RSR, NSE, R^2, and PBIAS values of model simulations during calibration were evaluated; the estimated and observed streamflow are graphically assessed for agreement. The model performance during the calibration and validation are presented in Table 3. The value of R^2 is 0.58 during calibration and 0.59 during validation. As these values are between 0.55 and 0.65, the performance was good as per Moriasi *et al.* (2007) criteria, especially at a daily time scale. Similarly, the value of NSE is 0.70 during calibration and 0.58 during validation. During calibration, the performance of the model was very good as it was more than 0.65 whereas during validation the performance was good as it was in the range of 0.55–0.65. Simulated streamflow is compared with the observed streamflow at the Kuniyil discharge station for 1995–2002 to check how well the simulated and observed streamflow are closely related, as shown in Figure 4. From Figure 4, it is clear that the day of simulated peak flow (i.e., 12 July 1997) closely matches the observed peak flow and the peak flow is 1740 m^3/s. The model predicts 20.66% less than the observed value when the peak flow is compared with simulated peak flow.

Table 3 | Performance indices of simulated and observed streamflow during calibration and validation

Performance measures	Calibration period	Validation period
RSR	0.54	0.66
NSE	0.71	0.56
R^2	0.58	0.59
PBIAS	−5.92	2.76

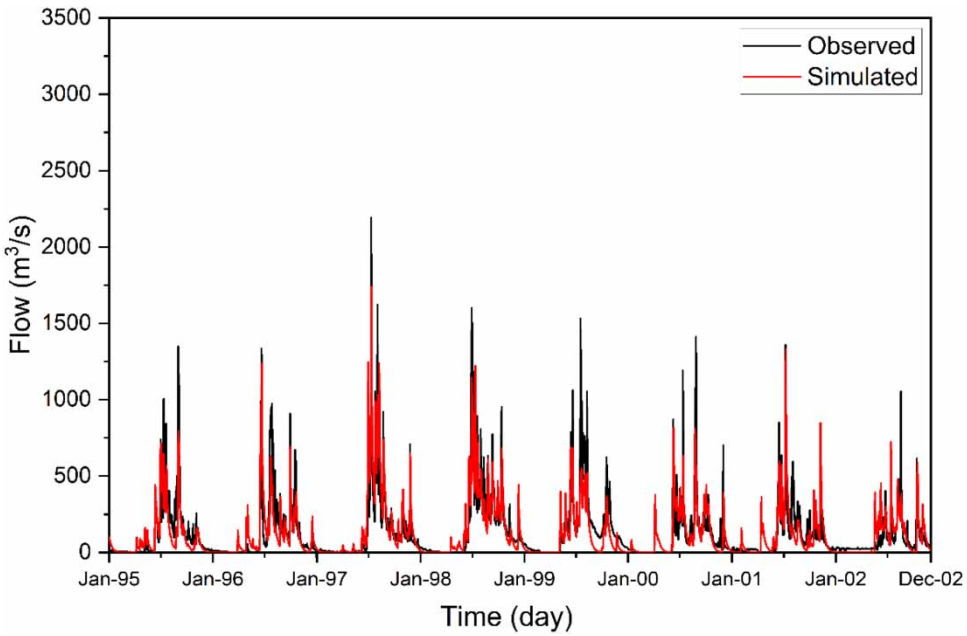

Figure 4 | Comparison of simulated and observed daily streamflow.

4.2. Future projections of streamflow

Once the model was properly calibrated and validated using the observed historical data for the baseline scenario, the model was used to simulate the streamflow for future climate scenarios by giving the precipitation projections as input. For the near future, simulated streamflow is higher for SSP5-8.5 than SSP2-4.5 as shown in Figure 5. Compared with the historical period, SSP2-4.5 shows a decreasing trend and SSP5-8.5 shows an increase for the near future with a reduction of 26.97% and an increase of 17.82%, respectively.

For mid-future, simulated streamflow is higher for SSP2-4.5 than SSP5-8.5 as shown in Figure 6. Compared with the historical period, SSP2-4.5 shows an increasing trend and SSP5-8.5 shows a decrease for mid-future with an increase of 56.76% and a reduction of 23.64%, respectively. For the far future, simulated streamflow is higher for SSP5-8.5 than SSP2-4.5 as shown in Figure 7. Compared with the historical period, SSP2-4.5 shows a decreasing trend and SSP5-8.5 shows an increase for the far future with a reduction of 47.40% and an increase of 29.18%, respectively.

4.3. Frequency analysis

The extreme flood frequency was calculated using the Gumbel distribution. The return periods of 25-, 50-, and 100-year of streamflow were taken into consideration for the flood inundation modelling under SSP2-4.5 and SSP5-8.5 scenarios during the near future (2031–2040), mid-future (2051–2060) and far future (2071–2080) as shown in Table 4. The maximum flood is recorded during mid-future, SSP2-4.5 for a 100-year return period. The 100-year maximum flood is increased by 41.2% for the mid-future for the SSP2-4.5 scenario. The maximum flood shows an increasing trend for the mid-future with respect to the baseline period. Similar results were also reported by Kim *et al.* (2023) for the Hangang and Geumgang basins in South Korea.

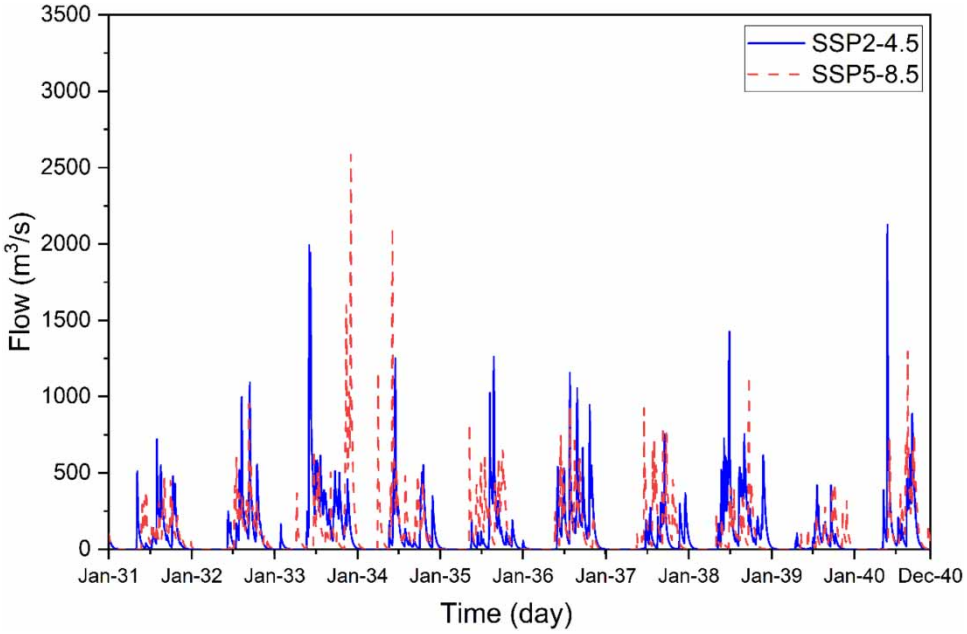

Figure 5 | Comparison of projected daily streamflow for near future under SSP2-4.5 and SSP5-8.5 scenarios.

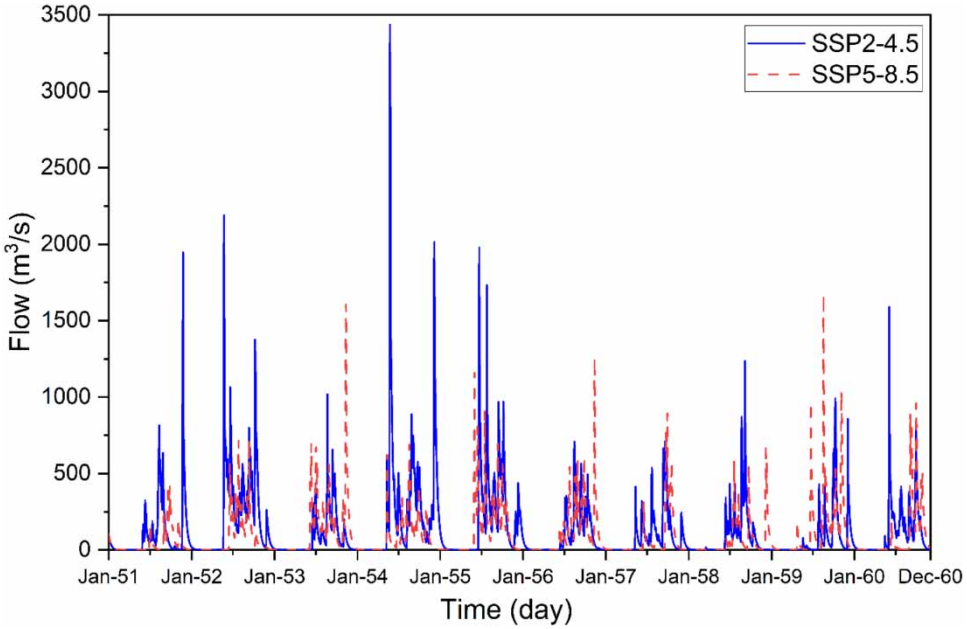

Figure 6 | Comparison of projected daily streamflow under SSP2-4.5 and SSP5-8.5 scenarios for mid-future.

4.4. Hydraulic modelling

In RAS Mapper, river banks, lines, and 2D mesh are first digitalized by using DEM. Cross-sections were created for every 1 km along the 32 km of the stretch. Following that, the geometric data were imported to HEC-RAS. Both the downstream and upstream boundary conditions are necessary for a mixed flow regime. By gradually changing Manning's coefficient from 0.03 to 0.08, the model was calibrated until the differences between the observed and the simulated values were within the acceptable ranges. When creating the flood inundation maps, the HEC-RAS model was set up to produce water levels and streamflow for 25-, 50-, and 100-year return periods. A total of 18 simulations were performed for different return periods and future periods. The output of the HEC-RAS model was viewed in the RAS Mapper before being exported to GIS to create flood

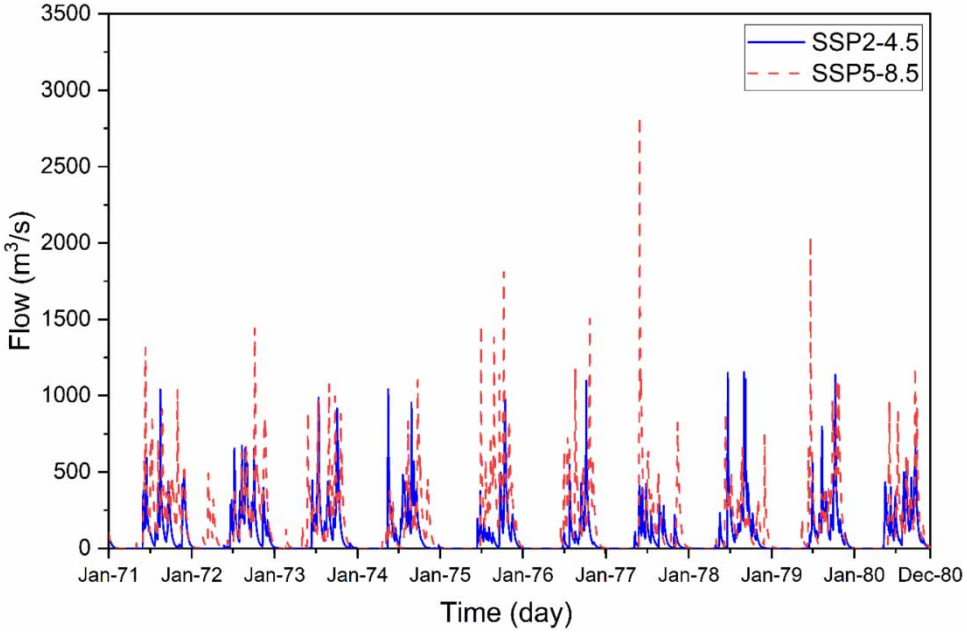

Figure 7 | Comparison of projected daily streamflow under SSP2-4.5 and SSP5-8.5 scenarios for far future.

Table 4 | Maximum flood (m^3/s) for various return periods under SSP2-4.5 and SSP5-8.5 scenarios

		Near future (2031–2040)		Mid-future (2051–2060)		Far future (2071–2080)	
Return period	**Base line period (1995–2004)**	**SSP2-4.5**	**SSP5-8.5**	**SSP2-4.5**	**SSP5-8.5**	**SSP2-4.5**	**SSP5-8.5**
25 years	2943	2748	3116	3983	2179	1619	3166
50 years	3325	3145	3623	4608	2484	1800	3595
100 years	3703	3540	4126	5229	2786	1981	4020

inundation maps. The maximum water surface elevations (WSE) are tabulated in Table 5. SSP5-8.5 shows an increased WSE of 0.68 m than SSP2-4.5 during the near future for 100-year return period. SSP5-8.5 shows an increased WSE of 2.81 m than SSP2-4.5 during mid-future for a 100-year return period. Similarly, SSP5-8.5 shows an increased WSE of 2.77 m than SSP2-4.5 during the far future, 100-year return period.

Table 5 | Maximum water surface elevation (m) for different return periods

	Near future		Mid-future		Far future	
Return period	**SSP2-4.5**	**SSP5-8.5**	**SSP2-4.5**	**SSP5-8.5**	**SSP2-4.5**	**SSP5-8.5**
25 years	16.65	17.16	18.22	15.81	14.80	17.22
50 years	17.19	17.80	18.90	16.27	15.14	17.77
100 years	17.70	18.38	19.52	16.71	15.49	18.26

Figure 8(a) represents the flood inundation boundary showing the places which are severely affected during mid-future for SSP2-4.5, 100-year return period which includes Vazhakkad, Kodiyathur, Kizhupparamba, Mavoor. A maximum of 19.52 m WSE occurred at Kizhupparamba. Figure 8(b) represents the flood inundation showing the places which are severely affected during the near future for SSP5-8.5 for 100-year return period which includes Vazhakkad, Kodiyathur, Kizhupparamba, Mavoor, Vilayil, and Cheekode. A maximum of 18.38 m WSE occurred at Cheekode. The inundated area is increased during SSP5-8.5 than SSP2-4.5 whereas during mid-future, 100 years, SSP2-4.5 shows maximum WSE than SSP5-8.5.

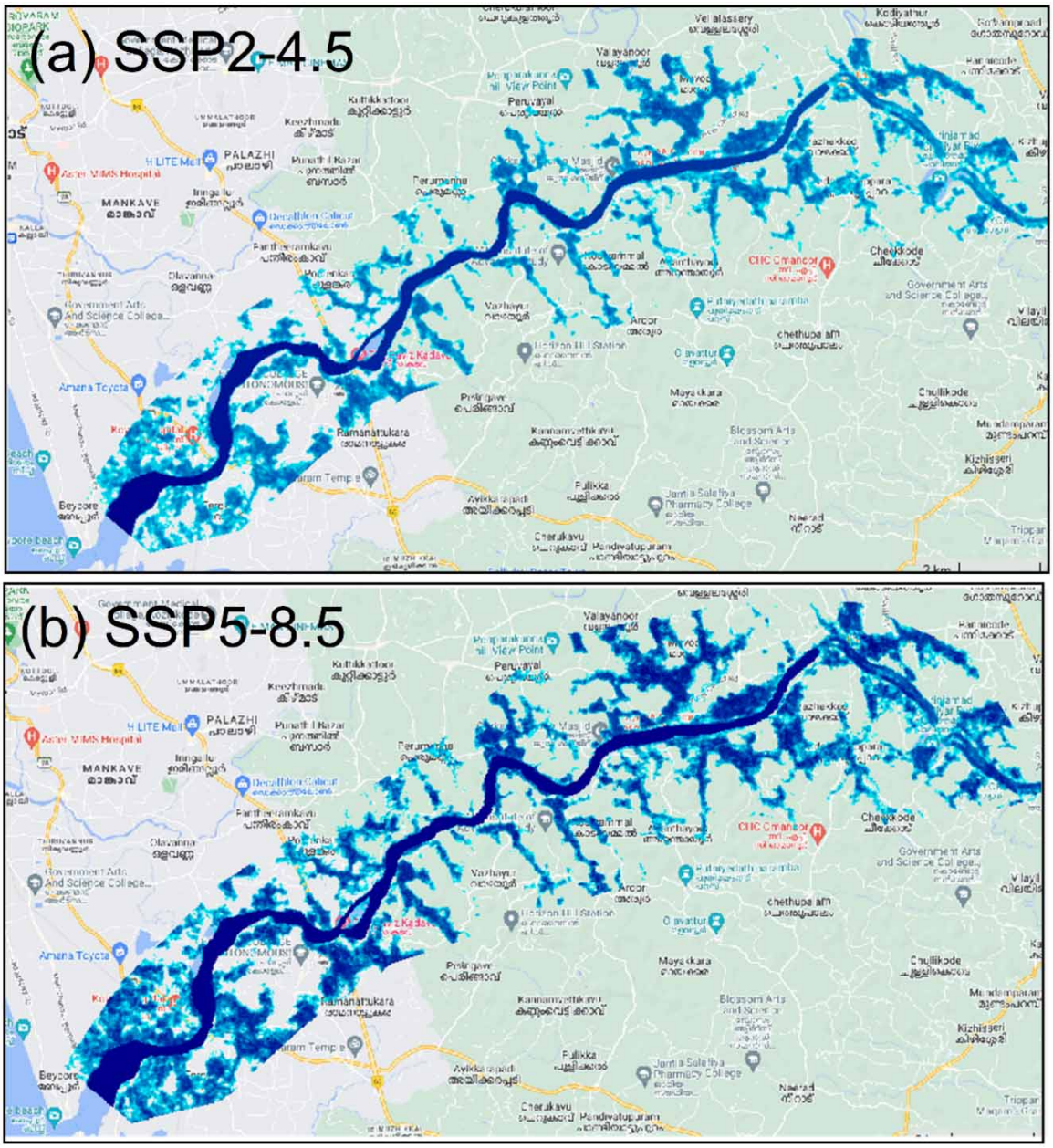

Figure 8 | Flood inundation boundary during (a) mid-future for SSP2-4.5, 100-year return period (b) near future for SSP5-8.5, 100-year return period.

5. CONCLUSIONS

In this study, the floodplains of the Chaliyar River basin are mapped using a hydrologic and hydraulic model for various climate change scenarios. Initially, a hydrologic model, HEC-HMS was developed to simulate the streamflow for various climate scenarios and time periods. Then, the frequency analyses were done to estimate the peak flows for different return periods. These peak flows were given as input to the HEC-RAS model to demarcate the floodplain regions. From the results, it is noticed that the HEC-HMS model has simulated the streamflow close to the observed values. The performance of the model is very good during calibration and good during validation. During the calibration of the HEC-HMS model, it is observed that time of concentration, initial deficit, maximum storage and constant rate are highly sensitive parameters as small change in the parameters affects the streamflow. For the near future and far future, simulated streamflow is higher for SSP5-8.5 than SSP2-4.5. But in the case of mid-future, simulated streamflow is higher for SSP2-4.5 than SSP5-8.5.HEC-RAS also has given good performance with R^2 at 0.63 and NSE at 0.61 during calibration. Vazhakkad, Kodiyathur, Kizhupparamba, Mavoor,

Vilayil, and Cheekode are vulnerable areas to flooding. A maximum of 19.52 m WSE occurred at Kizhupparamba during mid-future for SSP2-4.5 and 18.38 m occurred at Cheekode during the near future for SSP5-8.5 for a 100-year return period.

ACKNOWLEDGEMENT

Authors thankfully acknowledge the U.S. Geological Survey, India's Geo platform of ISRO (Bhuvan), Central Water Commission (CWC) and Indian Meteorological Society (IMD) for providing the necessary data required for this study.

DATA AVAILABILITY STATEMENT

Data cannot be made publicly available; readers should contact the corresponding author for details.

CONFLICT OF INTEREST

The authors declare there is no conflict.

REFERENCES

Abdessamed, D. & Abderrazak, B. 2019 Coupling HEC-RAS and HEC-HMS in rainfall–runoff modeling and evaluating floodplain inundation maps in arid environments: case study of Ain Sefra city, Ksour Mountain. SW of Algeria. *Environmental Earth Sciences* **78**(19), 586. https://doi.org/10.1007/s12665-019-8604-6.

Aich, V., Liersch, S., Vetter, T., Fournet, S., Andersson, J. C. M., Calmanti, S., van Weert, F. H. A., Hattermann, F. F. & Paton, E. N. 2016 Flood projections within the Niger River Basin under future land use and climate change. *Science of the Total Environment* **562**, 666–677. https://doi.org/10.1016/j.scitotenv.2016.04.021.

Assoumpta, M. & Aja, D. 2021 Flood forecasting using quantitative precipitation forecasts and hydrological modelling in the Sebeya catchment, Rwanda. *H_2Open Journal* **4**(1), 182–203. https://doi.org/10.2166/h2oj.2021.094.

Brunner, G. W. 2016 *HEC-RAS 6.0 Users Manual*. US Army Corps of Engineers, Institute for Water Resources, Hydrologic Engineering Center, Davis, CA, USA.

El Alfy, M. 2016 Assessing the impact of arid area urbanization on flash floods using GIS, remote sensing, and HEC-HMS rainfall–runoff modeling. *Hydrology Research* **47**(6), 1142–1160. https://doi.org/10.2166/nh.2016.133.

El-Naqa, A. & Jaber, M. 2018 Floodplain analysis using ArcGIS, HEC-GeoRAS and HEC-RAS in Attarat Um Al-Ghudran Oil Shale Concession Area, Jordan. *Journal of Civil & Environmental Engineering* **08**(05). https://doi.org/10.4172/2165-784X.1000323

Eum, H.-I., Sredojevic, D. & Simonovic, S. P. 2011 Engineering procedure for the climate change flood risk assessment in the Upper Thames River Basin. *Journal of Hydrologic Engineering* **16**(7), 608–612. https://doi.org/10.1061/(ASCE)HE.1943-5584.0000346.

Feldman, A. D. 2021 *Hydrologic Modeling System HEC-HMS User's Manual*. US Army Corps of Engineers, Institute for Water Resources, Hydrologic Engineering Center. Available from: https://users.auth.gr/vmarios/courses/DPMS/HEC-HMS/HEC-HMS%20User's%20Manual-v41-20210316_023441.pdf

Hamdan, A. N. A., Almuktar, S. & Scholz, M. 2021 Rainfall-runoff modeling using the HEC-HMS model for the Al-Adhaim River Catchment, Northern Iraq. *Hydrology* **8**(2), 58. https://doi.org/10.3390/hydrology8020058.

Kalra, A., Joshi, N., Baral, S., Nhuchhen Pradhan, S., Mambepa, M., Paudel, S., Xia, C. & Gupta, R. 2021 Coupled 1D and 2D HEC-RAS floodplain modeling of Pecos River in New Mexico. *World Environmental and Water Resources Congress* **2021**, 165–178. https://doi.org/10.1061/9780784483466.016.

Kim, S., Kwon, J.-H., Om, J.-S., Lee, T., Kim, G., Kim, H. & Heo, J.-H. 2023 Increasing extreme flood risk under future climate change scenarios in South Korea. *Weather and Climate Extremes* **39**(February), 100552.

Madhuri, R., Raja, Y. S. L. S., Raju, K. S., Punith, B. S. & Manoj, K. 2021 Urban flood risk analysis of buildings using HEC-RAS 2D in climate change framework. *H_2Open Journal* **4**(1), 262–275. https://doi.org/10.2166/h2oj.2021.111.

Mishra, B. K., Rafiei Emam, A., Masago, Y., Kumar, P., Regmi, R. K. & Fukushi, K. 2018 Assessment of future flood inundations under climate and land use change scenarios in the Ciliwung River Basin, Jakarta. *Journal of Flood Risk Management* **11**, S1105–S1115. https://doi.org/10.1111/jfr3.12311.

Mishra, V., Bhatia, U. & Tiwari, A. D. 2020a Bias-corrected climate projections for South Asia from coupled model intercomparison project-6. *Scientific Data* **7**(1), 338. https://doi.org/10.1038/s41597-020-00681-1.

Mishra, V., Bhatia, U. & Tiwari, A. D. 2020b Bias Corrected Climate Projections from CMIP6 Models for South Asia. Zenodo, (Data set). https://doi.org/10.5281/zenodo.3871316. Available from: https://zenodo.org/record/3987736 (accessed 2 August 2021).

Mohammed, K., Islam, A. K. M. S., Islam, G. M. T., Alfieri, L., Khan, M. J. U., Bala, S. K. & Das, M. K. 2018 Future floods in Bangladesh under 1.5°C, 2°C, and 4°C global warming scenarios. *Journal of Hydrologic Engineering* **23**(12), 04018050. https://doi.org/10.1061/(ASCE)HE.1943-5584.0001705.

Mohanty, M. P. & Simonovic, S. P. 2021 Changes in floodplain regimes over Canada due to climate change impacts: observations from CMIP6 models. *Science of the Total Environment* **792**, 148323. https://doi.org/10.1016/j.scitotenv.2021.148323.

Moriasi, D. N., Arnold, J. G., van Liew, M. W., Bingner, R. L., Harmel, R. D. & Veith, T. L. 2007 Model evaluation guidelines for systematic quantification of accuracy in watershed simulations. *Transactions of the ASABE* **50**(3), 885–900. https://doi.org/10.13031/2013.23153.

Motovilov, Y. G., Gottschalk, L., Engeland, K. & Rodhe, A. 1999 Validation of a distributed hydrological model against spatial observations. *Agricultural and Forest Meteorology* **98**, 257–277. https://doi.org/10.1016/S0168-1923(99)00102-1.

Nyaupane, N., Thakur, B., Kalra, A. & Ahmad, S. 2018 Evaluating future flood scenarios using CMIP5 climate projections. *Water* **10**(12), 1866. https://doi.org/10.3390/w10121866.

Rahman, M. M., Arya, D. S., Goel, N. K. & Dhamy, A. P. 2011 Design flow and stage computations in the Teesta River, Bangladesh, using frequency analysis and MIKE 11 modeling. *Journal of Hydrologic Engineering* **16**(2), 176–186. https://doi.org/10.1061/(ASCE)HE.1943-5584.0000299.

Raju, K. S. & Kumar, D. N. 2020 Review of approaches for selection and ensembling of GCMs. *Journal of Water and Climate Change* **11**(3), 577–599. https://doi.org/10.2166/wcc.2020.128.

Ramachandran, A., Palanivelu, K., Mudgal, B. V., Jeganathan, A., Guganesh, S., Abinaya, B. & Elangovan, A. 2019 Climate change impact on fluvial flooding in the Indian Sub-Basin: a case study on the Adyar Sub-Basin. *PLOS ONE* **14**(5), e0216461. https://doi.org/10.1371/journal.pone.0216461.

Reshma, C. & Arunkumar, R. 2023 Assessment of impact of climate change on the streamflow of Idamalayar River Basin, Kerala. *Journal of Water and Climate Change* **14**(7), 2133–2149. https://doi.org/10.2166/wcc.2023.456.

Roy, B., Khan, M. S. M., Islam, A. K. M. S., Mohammed, K. & Khan, M. J. U. 2021 Climate-induced flood inundation for the Arial Khan River of Bangladesh using open-source SWAT and HEC-RAS model for RCP8.5-SSP5 scenario. *SN Applied Sciences* **3**(6), 648. https://doi.org/10.1007/s42452-021-04460-4.

Sahoo, S. N. & Sreeja, P. 2017 Development of flood inundation maps and quantification of flood risk in an urban catchment of Brahmaputra River. *ASCE-ASME Journal of Risk and Uncertainty in Engineering Systems, Part A: Civil Engineering* **3**(1). https://doi.org/10.1061/AJRUA6.0000822

Shrestha, S. & Lohpaisankrit, W. 2017 Flood hazard assessment under climate change scenarios in the Yang River Basin, Thailand. *International Journal of Sustainable Built Environment* **6**(2), 285–298. https://doi.org/10.1016/j.ijsbe.2016.09.006.

Siddique, R. & Palmer, R. 2021 Climate change impacts on local flood risks in the U.S. Northeast: a case study on the Connecticut and Merrimack River Basins. *JAWRA Journal of the American Water Resources Association* **57**(1), 75–95. https://doi.org/10.1111/1752-1688.12886.

Ukumo, T. Y., Abebe, A., Lohani, T. K. & Edamo, M. L. 2022 Flood hazard mapping and analysis under climate change using hydro-dynamic model and RCPs emission scenario in Woybo River catchment of Ethiopia. *World Journal of Engineering*. https://doi.org/10.1108/WJE-07-2021-0410

Wen, K., Gao, B. & Li, M. 2021 Quantifying the impact of future climate change on runoff in the Amur river basin using a distributed hydrological model and CMIP6 GCM projections. *Atmosphere* **12**(12), 1560. https://doi.org/10.3390/atmos12121560.

First received 5 July 2023; accepted in revised form 14 September 2023. Available online 27 September 2023